Optimal Robust Control Based on State-Dependent Differential Riccati Equation with Application on Ducted Fan Aircraft

Mohamad Abbasi, Seyyed Sajjad Moosapour *, S. Saeedallah Mortazavi

Department of Electrical Engineering, Faculty of Engineering, Shahid Chamran University of Ahvaz, Ahvaz, Iran.
Email addresses: s.moosapour@scu.ac.ir
*Corresponding author

Received 24 March 2021, Revised day month year, Accepted day month year.

Abstract
In this paper, optimal robust controllers are developed for tracking control of a ducted fan engine of a thrust-vectored aircraft in the presence of external disturbances. First, by applying a nonlinear regulator based on the state-dependent differential Riccati equation (SDDRE) approach, an optimal control law is designed that is not robust against external disturbances. The second design, a VSC (variable structure control) with an NTV (nonlinear time-varying) sliding sector, is proposed. The sliding sector is a subset of the state space which is obtained by the SDDRE. As the final design, to guarantee the system's robustness against external disturbances and achieve optimal performance, a robust optimal sliding mode controller based on SDDRE (ROSMC) is designed, which integrates the sliding mode control (SMC) theory with the SDDRE approach. For each design, the global asymptotic stability is proved using the Lyapunov stability theorem. Also, the SDDRE is solved by a change of variable and converting it to a differential Lyapunov equation (DLE). Numerical simulations are presented considering different types of external disturbances and several scenarios. Simulation results show that ROSMC has stronger robustness and demonstrates optimal performance compared to SDDRE and VSC designs.

Keywords
Optimal, State-dependent differential Riccati equation (SDDRE), Variable structure control (VSC), Sliding mode, Ducted fan engine.

1. Introduction

Ducted fan engine is one of the primary parts of some jet aircraft that is a small flight control experimental model whose dynamics are representative of a VTOL (vertical take-off and landing) aircraft such as Harrier in hover mode or a thrust vectored aircraft such as X-31 or F18-HARV in forwarding flight mode [1]. Generally speaking, planar ducted fans have an equation of motion that follows the same nonlinearities as thrust-vectored aircraft [2]. Only a few studies have analyzed this particular system. In [3], comprehensive simulation analysis and nonlinear model have been presented for a ducted fan aircraft. A reliable fault-tolerant tracking controller has been developed for vertical take-off and landing aircraft [4].

Today, there are many nonlinear controller design techniques, each with its weaknesses and strengths. The range of application of most of them is limited because of their use of complex controllers such as predictive control, adaptive control, feedback linearization, sliding mode control, and sliding sector control (SSC), which leads to choosing efficient parameters such as performance and robustness.

This study aims to design controllers for a ducted fan engine in variable external disturbances using the SDRE approach. Recently, control engineers have become very interested in SDRE schemes as a practical approach for nonlinear control problems. It is a robust algorithm for handling nonlinearities in system states while at the same time offering an excessive degree of freedom due to state-dependent weighting matrices [5]. SDRE was initially proposed by Pearson [6]. Korayem and Nekoo [7] have investigated finite-time optimal control using the SDRE scheme for nonlinear time-varying systems with nonlinearity in the control input. An approximate solution for SDDRE has been introduced by Heydari and Balakrishnan [8]. A new type of SDDRE was introduced in [9] that provided an approximate closed-form solution for the finite horizon optimal control problem. An impact angle guidance based on SDDER has been presented for a missile in 2D and 3D spaces [10]. The linear-quadratic differential game theory has been applied to a spacecraft pursuit-evasion game in [11]. This theory was extended to derive a nonlinear control law using the state-dependent Riccati equation method.

One of VSC's main strengths is its ability to compensate for external disturbances and system uncertainties. In [12], an NTV sliding sector has been designed based on the SDDRE with forwarding integration and then using this NTV sliding sector, a VSC algorithm has been proposed for a class of NTV systems. Using VSC, a missile guidance law was proposed with a finite time sliding sector [13]. According to finite-time stability theory, the sliding sector was designed. In [14], a novel

VSC algorithm of event-triggered type, capable of dealing with a class of nonlinear uncertain systems, was proposed. In [15], Ship Electric Propulsion Speed Regulation System Based on Variable Structure Control and FPGA (Field-Programmable Gate Array) was designed and simulated.

SMC is considered an effective and robust control technique to handle sudden and significant changes in the system dynamics, uncertainties, and external disturbances and has been applied to many fields. In [16], a robust and optimal nonlinear controller based on an integral sliding surface was designed to neutralize the shimmy phenomenon's destructive effect in the nose landing gear of an aircraft. Two robust and optimal integral sliding mode controllers were proposed for position and attitude tracking of a rigid spacecraft in the presence of external disturbances [17]. Ref. [18] proposed a second-order sliding mode controller to solve a small quad rotor's position and altitude tracking problem. Ref. [1] proposed a controller combining backstepping control with fast terminal sliding mode control. Korayem et al. [19-20] integrated sliding mode control with the SDRE approach to design an optimal and robust controller.

Also, optimal robust control theory has been used in many other areas such as in delay systems [21, 22], power control systems such as DC-DC boost converter [23], and wind turbine [24] intelligent systems such as neural networks [25] and fuzzy control system [24]. Additionally, in [26], a tracking controller has been developed using the SDRE method, and the output tracking design has been studied using the SDRE approach in [27]. Moreover, in [28], based on the SDRE technique, a new method has been proposed to design nonlinear observers in a class of networked control systems. Finally, in [29], a model reference adaptive control based on SDRE for finite duration cancer treatment has been presented by using a mixed therapy.

The main contribution of this paper can be described in the following:

1- The main reference in this study is [1]. A sliding mode controller based on backstepping theory has been designed for the ducted fan engine system. In this paper, by applying a nonlinear regulator based on the SDDRE method, an optimal non-robust controller is designed for a Ducted Fan engine of a Thrust-Vectored Aircraft derived from [1]. SDDRE is solved by changing the variable and converting it to a Differential Lyapunov Equation (DLE).
2- In [12], a variable structure controller (VSC) with a nonlinear time-varying sliding sector is proposed for the scalar systems. We have extended that to multi-input multi-output (MIMO) systems and integrated it with the SDDRE technique to optimal performance. The SDDRE obtains the sliding sector. Implementing the proposed method on the Ducted Fan engine improves the simulation results compared to [1].
3- To achieve optimal performance and system robustness against external disturbances, a robust optimal sliding mode controller based on SDDRE (ROSMC) integrates SMC with the SDDRE approach. Regarding the importance of optimality and robustness, we can have a trade-off by changing the design parameters. The simulation results are significantly improved in comparison with [1].
4- For each design, the global asymptotic stability is proved using the Lyapunov stability theorem.

The rest of this paper is organized as follows. In Section 2, the formulation of a ducted fan engine for controlling a thrust-vectored aircraft is presented. In section 3, the nonlinear optimal SDDRE feedback control approach and approximate solution for SDDRE are discussed. A new variable structure control based on the nonlinear time-varying (NTV) sliding sector is presented in Section 4. Robust optimal SMC (ROSMC) is shown in Section 5. Simulation results are provided in Section 6. Finally, conclusions are presented in Section 7.

2. Problem Formulation of a Ducted Fan Engine

In a ducted fan, a mechanical fan is installed into a channel or cylinder-shaped duct to provide propulsion. In Fig. 1, an engine with a ducted fan is shown as a simple planar model. There is a pair of flaps at the bottom of the ducted fan. When you activate them, the thrust can be vectored from left to right or vice versa [1]. For extracting dynamic equations of the ducted fan, let x be the horizontal axis, y be the vertical axis and ϕ be the angular position of a point on the central axis of the fan. We assume that the influential forces on the ducted fan engine are F_1 and F_2 , which act perpendicular and parallel respectively to the central axis of the fan. Also, it is assumed that F_1 acts at a distance L from the center of mass. Naturally, F_1 is much less than F_2 . Another assumption is that the drag and friction terms are represented as viscous friction [1].

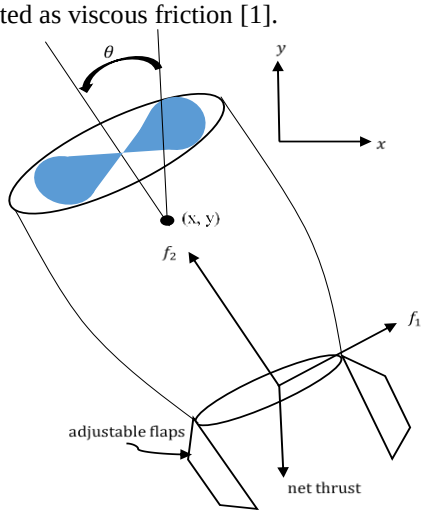

Fig. 1. Planer schematic of ducted fan engine for controlling aircraft

According to Fig. 1 and by applying Newton's second law and taking each force's direction into account, dynamic equations of the system are obtained as follows:

$$\begin{aligned} m_x \ddot{x} &= -\eta \dot{x} + F_1 \cos\phi - F_2 \sin\phi \\ m_y \ddot{y} &= -\eta \dot{y} + F_1 \sin\phi + F_2 \cos\phi - m_g g \\ J\ddot{\phi} &= LF_1 \end{aligned} \tag{1}$$

Where η is viscous friction coefficient, L is the distance from the center of mass, the constant parameters m_y, m_x, g and J are inertial masses in directions y and x, the gravitational constant and the moment of inertia, respectively. The term $m_g g$ is the weight force. By redefining the inputs $u_1 = F_1$ and $u_2 = -m_g g + F_2$, the nonlinear equations of motion for the ducted fan engine are redefined as

$$\begin{aligned}
\ddot{x} &= -\frac{m_g g \sin\phi}{m_x \phi}\phi - \frac{\eta}{m_x}\dot{x} + \frac{\cos\phi}{m_x}(u_1 + d_1) \\
&\quad -\sin\phi(u_2 + d_2)/m_x \\
\ddot{y} &= \frac{m_g g\left(\cos\phi - 1\right)}{m_y \phi}\phi - \frac{\eta}{m_y}\dot{y} + \frac{\sin\phi}{m_y}(u_1 + d_1) \\
&\quad +\cos\phi(u_2 + d_2)/m_y \\
\ddot{\phi} &= (L/J)u_1
\end{aligned} \tag{2}$$

Where parameters d_1 and d_2 are unknown functions representing external disturbances. In order to design the SDDRE feedback control law and ROSMC, the system equations should be transformed into the State-Dependent Coefficient (SDC) form as follows:

$$\begin{aligned}
\dot{\mathbf{x}} &= A(\mathbf{x})\mathbf{x}(\mathrm{t}) + B(\mathbf{x})\left[\mathbf{u} + \mathbf{d}\right] \\
\mathbf{y} &= C(\mathbf{x})\mathbf{x}
\end{aligned} \tag{3}$$

Where $A(\mathbf{x}) \in R^{n\times n}$ and $\mathrm{B}(\mathbf{x}) \in R^{n\times m}$ are states and input matrices, respectively, they can be linear or nonlinear functions of state variables. $\mathbf{d} = \begin{bmatrix} d_1 & d_2 \end{bmatrix}^T$ is the external disturbance vector. As a result, from (2) and by defining the state variables $\mathbf{x}$ and outputs $\mathbf{y}$ as follow, dynamic equations of the ducted fan engine in the SDC form can be given as follows

$$\begin{aligned}
\dot{\mathbf{x}} &= \begin{bmatrix}
0 & 0 & 0 & 1 & 0 & 0 \\
0 & 0 & 0 & 0 & 1 & 0 \\
0 & 0 & 0 & 0 & 0 & 1 \\
0 & 0 & -\frac{m_g g}{m_x}\frac{\sin\phi}{\phi} & -\frac{\eta}{m_x} & 0 & 0 \\
0 & 0 & \frac{m_g g}{m_y}\frac{\left(\cos\phi - 1\right)}{\phi} & 0 & -\frac{\eta}{m_y} & 0 \\
0 & 0 & 0 & 0 & 0 & 0
\end{bmatrix}\mathbf{x} \\
&\quad + \begin{bmatrix}
0 & 0 \\ 0 & 0 \\ 0 & 0 \\
\frac{\cos\phi}{m_x} & -\frac{\sin\phi}{m_x} \\
\frac{\sin\phi}{m_y} & \frac{\cos\phi}{m_y} \\
\frac{L}{J} & 0
\end{bmatrix}\begin{bmatrix} u_1 + d_1 \\ u_2 + d_2 \end{bmatrix}, \quad \mathbf{x} = \begin{bmatrix} x \\ y \\ \phi \\ \dot{x} \\ \dot{y} \\ \dot{\phi} \end{bmatrix} \\
\dot{\mathbf{x}}(\mathrm{t}) &= A(\mathbf{x})\mathbf{x}(t) + B(\mathbf{x})\left[\mathbf{u} + \mathbf{d}\right] \\
\mathbf{y} &= \begin{bmatrix} 1 & 0 & 0 & 0 & 0 & 0 \\ 0 & 1 & 0 & 0 & 0 & 0 \end{bmatrix}\mathbf{x}(\mathrm{t}) = C(\mathbf{x})\mathbf{x}(\mathrm{t})
\end{aligned} \tag{4}$$

The control objective of the system is to regulate state variables $\mathbf{x}$ and outputs $\mathbf{y}$ so that they reach zero value. As it can be seen, (4) has the same form as (3).

Remark 1. For multivariable problems, such as the given system, the SDC parameterization is not unique. A proper choice of $A(\mathbf{x})$, such as the selected $A(\mathbf{x})$ in (3), plays a significant role in affecting the controllability of the resulting parameterized pair $\{A(\mathbf{x}), \mathrm{B}(\mathbf{x})\}$. The matrix $A(\mathbf{x})$ presented in (4) satisfies this condition. Also, these additional degrees of freedom provide design flexibility that can be used to enhance performance or effect trade-offs between robustness, optimality, stability, performance, and disturbance rejection.

3. SDDRE Control

3.1. Nonlinear regulator based on SDDRE

Assumption 1. Considering system (3), the pairs $[A(\mathbf{x}), B(\mathbf{x})]$, and $[\mathrm{A}(\mathbf{x}), C(\mathbf{x})]$ are supposed to be completely controllable and observable, respectively. For the present system with the selected $A(\mathbf{x})$ and $B(\mathbf{x})$, this condition is satisfied.

Assumption 2. It is assumed that all state variables are measurable.

One of the design goals of optimal control is minimizing the finite time quadratic performance index, which is described as follows [7]:

$$J = \frac{1}{2}\mathbf{x}^T(t_f)F(\mathbf{x})x(t_f) + \frac{1}{2}\int_{t_0}^{t_f}\left(\mathbf{x}^T Q\mathbf{x} + \mathbf{u}^T R\mathbf{u}\right)dt \tag{5}$$

Where $F(\mathbf{x})$ and $Q(\mathbf{x})$ are $n\times n$ symmetric positive semi-definite state weighting matrices, and $R(\mathbf{x})$ is a $m\times m$ symmetric positive definite input weighting matrix. With assumption 1, and according to the SDDRE approach, the optimal control law is given by [7]

$$\begin{aligned}
\mathbf{u}_{SDDRE} &= -R^{-1}(\mathbf{x})B^T(\mathbf{x})P(\mathbf{x},t)\mathbf{x}(t) \\
&= -K(\mathbf{x},t)\mathbf{x}(t) = \begin{bmatrix} -\sum_{i=1}^{6} k_{1i}\mathbf{x}_i \\ -\sum_{i=1}^{6} k_{2i}\mathbf{x}_i \end{bmatrix}
\end{aligned} \tag{6}$$

Where $K(\mathbf{x},t) = R^{-1}(\mathbf{x})B^T(\mathbf{x})P(\mathbf{x},t)$ is the well-known Kalman gain matrix, k_{ij} with $i = 1,\cdots 6$ and $j = 2$ is the element of the matrix $K(\mathbf{x},t)$, and $P(\mathbf{x},t)$ is the $n\times n$ symmetric positive definite matrix obtained by solving the following SDDRE [7]:

$$\dot{P} = -PA - A^T P + PBR^{-1}B^T P - Q \tag{7}$$

Considering the final condition $P(\mathbf{x}(t_f), t_f) = F$, the solution of (7) will be available. Consequently, the optimal closed-loop states are obtained by solving (8):

$$\dot{\mathbf{x}}(t) = \left[A(\mathbf{x}) - B(\mathbf{x})R^{-1}(\mathbf{x})B(\mathbf{x})P(x,t)\right]\mathbf{x}(t) \tag{8}$$

Fig. 2 shows a process of the SDDRE technique.

Remark 2. The computational simplicity of this control algorithm makes real-time problems practically realizable. However, the SDRE feedback has only been applied as a regulator-type control.

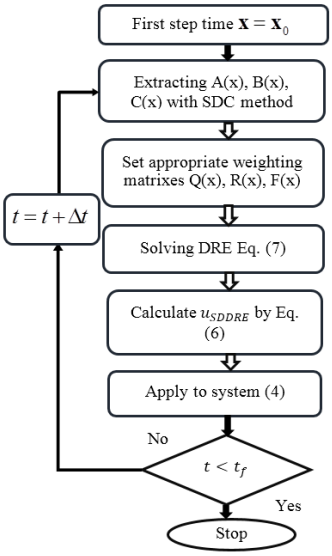

Fig. 2. Process of the SDDRE technique

3.2. Approximate Solution for SDDRE based on Lyapunov Technique

Equation (7) can be solved by different approaches such as power series, exact solution, online control, Backward Integration (BI), and an approximate solution technique [7]. The SDDRE or Differential Riccati Equation (DRE) is a function of variables $\mathbf{x}$ and t. In each sample time, future values of the state variables are not available; hence, the values of SDC matrices cannot be obtained. Consequently, (7) cannot be solved with the final boundary condition $P(\mathbf{x}(t_f), t_f)$ by backward integration approach from final time t_f to the initial time t_0. In this paper, an approximate solution based on the variable change is utilized to overcome this difficulty and solve SDDRE (7). In this approach, SDDRE (7) is converted to a nonlinear DLE such that it provides a solution for the Lyapunov equation in closed form for each time interval. The approximate solution for solving SDDRE can be found in [9].

4. VSC based on NTV Sliding Sector

Before designing the VSC for the system, the following assumption and remarks are stated.

Assumption 3. The control objective of our problem is to regulate state variables $\mathbf{x}$ and $\mathbf{y}$ to zero. Hence, we ignore the third state variable ϕ. For this purpose, we apply a saturation on ϕ with the magnitude $\pi/20$ rad.

Remark 3. According to assumption 3, since ϕ is limited by a saturation function between $-\pi/20$ and $+\pi/20$ rad, one can assume $\cos(\phi) \simeq 1$ and $\sin(\phi) \simeq 0$, with an acceptable approximation. Consequently, the matrix $B(\mathbf{x},t)$ converts to a constant diagonal matrix $B = \text{diag}(1/m_x, 1/m_y)$. As a result, the time derivative of matrix B equals zero. To design the VSC and prove the stability, we need matrix B to be constant. Without that, designing and proving the stability of the VSC is impossible.

Essentially, the control law based on the sliding sector comprises two different terms with different structures. The first term is to achieve optimal performance, the same as control law based on SDDRE. The second term is based on the sliding sector, and its goal is to make the system robust against external disturbances. Ignoring the external disturbance $\mathbf{d}$ in the system (4), assume that $\mathbf{u} = \mathbf{u}_{\text{con}} = \mathbf{u}_{\text{SDDRE}}$ is the primary control input for the ducted fan system. The control law is chosen to compensate for external disturbances $\mathbf{d}$ in (4), in the form of:

$$\mathbf{u} = \mathbf{u}_{\text{con}} + \mathbf{u}_{\text{dis}} \tag{9}$$

where $\mathbf{u}_{\text{dis}} = \begin{bmatrix}\mathbf{u}_{\text{dis1}} & \mathbf{u}_{\text{dis2}}\end{bmatrix}^T$ is the discontinuous control input which should be designed to compensate for external disturbances. Substituting (9) and (***6***) into (4) yields

$$\begin{aligned}\dot{\mathbf{x}} &= A(\mathbf{x},t)\mathbf{x} + B(\mathbf{x},t)\left[\mathbf{u} + \mathbf{d}\right] \\ &= A(\mathbf{x},t)\mathbf{x} - B(\mathbf{x},t)K(\mathbf{x})\mathbf{x} + B(\mathbf{x},t)\left[\mathbf{u}_{\text{dis}} + \mathbf{d}\right] \\ &= \left[\mathrm{A}(\mathbf{x},t) - B(\mathbf{x},t)K(\mathbf{x})\right]\mathbf{x} + B(\mathbf{x},t)\left[\mathbf{u}_{\text{dis}} + \mathbf{d}\right] \\ &= A_{\text{new}}(\mathbf{x},t)\dot{\mathbf{x}} + B(\mathbf{x},t)\left[\mathbf{u}_{\text{dis}} + \mathbf{d}\right]\end{aligned} \tag{10}$$

Now, to design the second term of the controller $\mathbf{u}_{\text{dis}}$, a sliding sector must be designed. An NTV sliding sector for system (10) is considered as follows:

$$S(\mathbf{x},t) = \left\{\mathbf{x} \,\middle|\, \|\boldsymbol{\sigma}(\mathbf{x},t)\| \le \|\delta(\mathbf{x},t)\|, \mathbf{x} \in R^n, t \in R^+\right\} \tag{11}$$

where $\delta(\mathbf{x},t)$ and $\boldsymbol{\sigma}(\mathbf{x},t)$ in (11) are obtained as follows:

$$\begin{aligned}&\boldsymbol{\sigma}(\mathbf{x},t) = S(\mathbf{x},t)\mathbf{x}, \;\; S(\mathbf{x},t) = B^T(\mathbf{x},t)P(\mathbf{x},t) \\ &\|\delta(\mathbf{x},t)\| = \sqrt{\mathbf{x}^T\Delta(\mathbf{x},t)\mathbf{x}} \\ &\Delta(\mathbf{x},t) = Q(\mathbf{x},t) - R(\mathbf{x},t) \ge 0 \\ &\mathbf{x}^T Q(\mathbf{x},t)\mathbf{x} = -\delta^2(\mathbf{x},t) - \mathbf{x}^T R(\mathbf{x},t)\mathbf{x}\end{aligned} \tag{12}$$

where $R(\mathbf{x},t)$ is a positive matrix, $Q(\mathbf{x},t) \in R^n$ is a symmetric positive definite matrix, and $P(\mathbf{x},t)$ is a matrix that plays a significant role in the design of the sliding sector and is determined by the following equation:

$$\begin{aligned}\dot{P}(\mathbf{x},t) = &-P(\mathbf{x},t)A_{\text{new}}(\mathbf{x},t) - A_{\text{new}}^T(\mathbf{x},t)P(\mathbf{x},t) \\ &+P(\mathbf{x},t)B(\mathbf{x},t)B^T(\mathbf{x},t)P(\mathbf{x},t) - Q(\mathbf{x},t)\end{aligned} \tag{13}$$

Inside the defined sector, a positive definite function $V(\mathbf{x},t)$ should be introduced as the Lyapunov function candidate to satisfies the condition $\dot{V}(\mathbf{x},t) \le -cV^{\alpha}(\mathbf{x},t)$ where $0 < \alpha < 1$ and $c > 0$. These mentioned conditions on Lyapunov function guarantee the stability inside the sliding sector. The VSC controller consists of two parts: one part for the inside of the sliding sector and another for the outside. In the following two subsections, we design the VSC law for each region.

4.1. The Variable Structure Control Law for inside the Sector

Theorem 1. If the following VSC law is used for inside the sliding sector defined by (11), then the sector will be a so-called "finite time" sliding sector.

$$\begin{aligned}\mathbf{u}_{\text{dis\_in}} &= -\left(r_1 + r_2\left\|S(\mathbf{x},t)\mathbf{x}\right\|^{2\alpha-1}\right)\text{sgn}(S(\mathbf{x},t)\mathbf{x}) \\ &= -\left(r_1 + r_2\left\|\boldsymbol{\sigma}(\mathbf{x},t)\right\|^{2\alpha-1}\right)\text{sgn}(\boldsymbol{\sigma}(\mathbf{x},t)) \\ &= -k\,\text{sgn}(\boldsymbol{\sigma}(\mathbf{x},t))\end{aligned} \tag{14}$$

in which sgn(·) is the sign function. r_1, r_2 and α are constant parameters, and they are limited by the following conditions:

$$r_1 \geq \|\mathbf{d}\|, \quad r_2 \geq \frac{c\lambda_{\max}\left(P(\mathbf{x},t)\right)}{2\lambda_{\min}\left(S^T(\mathbf{x},t)S(\mathbf{x},t)\right)}, \qquad 0<\alpha<1$$

Where $\lambda_{\max}(\cdot)$ and $\lambda_{\min}(\cdot)$ denote the maximum and minimum singular values of any matrices, respectively, and c is a real positive constant.

Proof. For the solution $P(\mathbf{x},t)$ of (13), a candidate for the Lyapunov function is considered as follows:

$$V(\mathbf{x},t)=\mathbf{x}^T P(\mathbf{x},t)\mathbf{x}>0 \tag{15}$$

Its derivative along the system trajectories (***4***) is given by

$$\begin{aligned}\dot{V}(\mathbf{x},t) &= 2\mathbf{x}^T P(\mathbf{x},t)B(\mathbf{x},t)(\mathbf{u}+\mathbf{d})+\\ &\mathbf{x}^T\left(\dot{P}(\mathbf{x},t)+A^T(\mathbf{x},t)P(\mathbf{x},t)+P(\mathbf{x},t)A(\mathbf{x},t)\right)\mathbf{x}\\ &=+2\boldsymbol{\sigma}^T(\mathbf{x},t)(\mathbf{u}+\mathbf{d})-\mathbf{x}^T R(\mathbf{x},t)\mathbf{x}\\ &-\delta^2(\mathbf{x},t)+\boldsymbol{\sigma}^2(\mathbf{x},t)\\ &\leq 2\boldsymbol{\sigma}^T(\mathbf{x},t)(\mathbf{u}+\mathbf{d})\end{aligned} \tag{16}$$

By substituting the VSC law (14) into (16), we have:

$$\begin{aligned}\dot{V}(\mathbf{x},t) &\leq 2\boldsymbol{\sigma}^T(\mathbf{x},t)\Big[-\big(r_1\\ &+r_2\|\boldsymbol{\sigma}(\mathbf{x},t)\|^{2\alpha-1}\big)\mathrm{sgn}(\boldsymbol{\sigma}(\mathbf{x},t))+\mathbf{d}\Big]\\ &\leq -2r_2\|\boldsymbol{\sigma}(\mathbf{x},t)\|^{2\alpha}\end{aligned} \tag{17}$$

According to the property of singular values, we have

$$\|\sigma\|^2 \geq \lambda_{\min}\left(S^T S\right)\|\mathbf{x}\|^2 \tag{18}$$

$$V(x,t)\leq \lambda_{\max}(P)\|\mathbf{x}\|^2 \tag{19}$$

From equations (18) and (19), the following inequality is obtained:

$$\|\boldsymbol{\sigma}\|^2 \geq \frac{\lambda_{\min}\left(S^T S\right)}{\lambda_{\max}(P)}V(\mathbf{x},t) \tag{20}$$

Substituting equation (20) into (17) yields

$$\dot{V}(\mathbf{x},t)\leq -2r_2\left(\frac{\lambda_{\min}(S^T S)}{\lambda_{\max}(P)}\right)^{\alpha}V^{\alpha}(\mathbf{x},t)=-cV^{\alpha}(\mathbf{x},t) \tag{21}$$

Consequently, the region characterized by (11) is a finite-time sliding sector.

4.2. The VSC Law for outside the Sliding Sector

The second part of designing the VSC law is related to the outside of the sliding sector.

Theorem 2. A control signal is provided for outside the sliding sector by

$$\begin{aligned}\mathbf{u}_{dis} &= -H^{-1}\left[G+(r_3H+r_4\|S(\mathbf{x},t)x\|^{2\beta-1})\mathrm{sgn}(S(\mathbf{x},t)\mathbf{x})\right]\\ &= -H^{-1}\left[G+\left(r_3H+r_4\|\boldsymbol{\sigma}(\mathbf{x},t)\|^{2\beta-1}\right)\mathrm{sgn}(\boldsymbol{\sigma}(\mathbf{x},t))\right]\end{aligned} \tag{22}$$

Where $G=B^T\dot{P}(\mathbf{x},t)\mathbf{x}+B^T P(\mathbf{x},t)A(\mathbf{x},t)\mathbf{x}$ and the matrix $H=B^T P(\mathbf{x},t)B$ is positive and invertible, $r_3>\|\mathbf{d}\|$, $r_4>0$ and $0<\beta<1$ are constants. With this control law, the trajectories of the system states will converge to the sliding sector at a finite time.

Proof. By defining the new Lyapunov function $V(\mathbf{x},t)=\boldsymbol{\sigma}^T(\mathbf{x},t)\boldsymbol{\sigma}(\mathbf{x},t)/2$ and differentiating it, we have:

$$\dot{V}(\mathbf{x},t)=\boldsymbol{\sigma}^T(\mathbf{x},t)\dot{\boldsymbol{\sigma}}(\mathbf{x},t) \tag{23}$$

As a result, we have:

$$\dot{\boldsymbol{\sigma}}(x,t)=\frac{d}{dt}\left(S(\mathbf{x},t)\mathbf{x}\right)=G+H\left(\mathbf{u}+\mathbf{d}\right) \tag{24}$$

Substituting equations (22) and (24**)** into (23) yields

$$\begin{aligned}\dot{V}(\mathbf{x},t) &= \boldsymbol{\sigma}^T(\mathbf{x},t)\Big\{G+H\Big[-H^{-1}\big(G+\\ &\quad r_3H\mathrm{sgn}\left(\boldsymbol{\sigma}(\mathbf{x},t)\right)+\\ &\quad r_4\|\boldsymbol{\sigma}(\mathbf{x},t)\|^{2\beta-1}\mathrm{sgn}\left(\boldsymbol{\sigma}(\mathbf{x},t)\right)\big)+d\Big]\Big\}\\ &\leq -r_4\|\boldsymbol{\sigma}(\mathbf{x},t)\|^{2\beta-1}\boldsymbol{\sigma}^T(\mathbf{x},t)\mathrm{sgn}\left(\boldsymbol{\sigma}(\mathbf{x},t)\right)\\ &\leq -r_4V^{\beta}(\mathbf{x},t)\end{aligned} \tag{25}$$

That implies that the system's state variables will move to the inside of the sliding sector at a finite time.

4.3. The Final Variable Structure Control Law

As a result, the overall VSC law can be written as a combination of two parts as follows:

$$\begin{aligned}\mathbf{u}_{\mathrm{VSC}} &= \mathbf{u}_{\mathrm{SDDRE}}+\mathbf{u}_{\mathrm{dis}}\\ &=\begin{cases}\mathbf{u}_{\mathrm{SDDRE}}-(r_1+\\ r_2\|\boldsymbol{\sigma}(x,t)\|^{2\alpha-1})\mathrm{sgn}\left(\boldsymbol{\sigma}(x,t)\right) & \forall x\in S\\ \mathbf{u}_{\mathrm{SDDRE}}-H^{-1}\big[G+\big(r_3H+\\ r_4\|\boldsymbol{\sigma}(\mathbf{x},t)\|^{2\beta-1}\big)\mathrm{sgn}(\boldsymbol{\sigma}(\mathbf{x},t))\big] & \forall x\notin S\end{cases}\end{aligned} \tag{26}$$

The block diagram of the designed VSC is presented in Fig. 3.

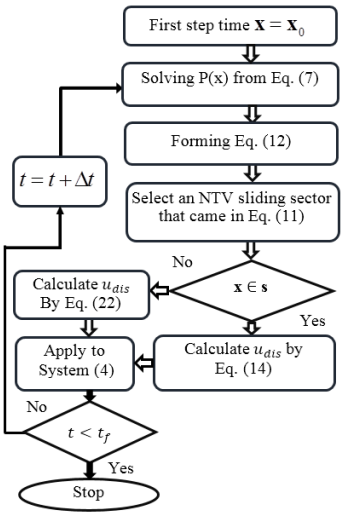

Fig. 3. Flowchart of the proposed VSC.

5. ROBUST OPTIMAL SLIDING MODE CONTROL

The main objective of this section is to design an optimal robust SMC or ROSMC law for a ducted fan engine system, such that the quadratic performance index (5) is minimized and the system is robust against uncertainties.

Assumption 4. There exist unknown constants $\gamma_0>0$ and $\gamma_1>0$ such that in the ducted fan engine described in (3) $\|d\|\leq\gamma_1\|\mathbf{x}(t)\|+\gamma_0$. Here, $\|.\|$ represents the Euclidean norm.

The overall control law is chosen to overcome and compensate for the uncertainties of the system (3), as follows:

$$\mathbf{u} = \mathbf{u}_{con} + \mathbf{u}_{dis} \tag{27}$$

where $\mathbf{u}_{con}$ is the optimal and continuous part, and $\mathbf{u}_{dis}$ is the discontinuous part of the control law. Considering system (3), an integral sliding surface is chosen as,

$$\begin{aligned} s(t, x(t)) &= M\left[x(t) - x(0)\right] \\ &- \int_0^t \left[MA(x(t)) - Z(x(t))K(x(t))\right] x(\tau) d\tau, \end{aligned} \tag{28}$$

where $M \in R^{m \times n}$ is an arbitrary constant matrix which must satisfy the non-singularity condition of matrices $Z(\mathbf{x}) = MB(\mathbf{x})$. Also, we have $K(\mathbf{x}) = R^{-1}(\mathbf{x})B^T(\mathbf{x})P(\mathbf{x})$ and $s(0, \mathbf{x}(0)) = 0$. Using (28), the continuous or equivalent control law can be derived as follows,

$$\mathbf{u}_{eq} = \mathbf{u}_{SDDRE} = -R^{-1}(\mathbf{x})B^T(\mathbf{x})P(\mathbf{x})\mathbf{x}(t) = -K(\mathbf{x})\mathbf{x}(t) \tag{29}$$

The necessary condition for stability of (3) is $s^T \dot{s} < 0$. Thus, the ROSMC is described by

$$\begin{aligned} \mathbf{u}_{con} &= \mathbf{u}_{eq} = -R^{-1}(\mathbf{x})B^T(\mathbf{x})P(\mathbf{x})\mathbf{x}(t) = -K(\mathbf{x})\mathbf{x}(t) \\ \mathbf{u}_{dis} &= -Z^{-1}(\mathbf{x})\left(\eta + \gamma_0 \left\|Z(\mathbf{x})\right\| + \gamma_1 \left\|Z(\mathbf{x})\right\| \left\|\mathbf{x}\right\|\right) \mathrm{sgn}(s) \\ \mathbf{u} &= \mathbf{u}_{con} + \mathbf{u}_{dis} \end{aligned} \tag{30}$$

where $\eta > 0$ is a real constant, $Z(\mathbf{x})$ should be invertible, and $\mathrm{sgn}(s)$ is a vector function defined by

$$\mathrm{sgn}(s) = \left[\mathrm{sgn}(s_1), \mathrm{sgn}(s_2), ..., \mathrm{sgn}(s_m)\right]^T.$$

Theorem 3. Consider the uncertain system (3). Assume that all conditions mentioned in Assumption 4 hold. In addition, define the sliding surface as (28) and the control law as (30). Therefore, the control law for system trajectories can force them to reach the sliding surface within a finite time and remain there after that.

Proof. The time derivative of the sliding surface (28) is calculated as follows

$$\begin{aligned} \dot{s} &= M\dot{x}(t) - MA(\mathbf{x})\mathbf{x} + Z(\mathbf{x})K(\mathbf{x})\mathbf{x} \\ &= Z(\mathbf{x})\left(\mathbf{u} + \mathbf{d}\right) + Z(\mathbf{x})K(\mathbf{x})\mathbf{x} \end{aligned} \tag{31}$$

Choosing $V = (1/2)s^T s$ as a Lyapunov function candidate and substituting the control law (30) into (31) yields

$$\begin{aligned} \dot{V} &= -s^T\left[Z(\mathbf{x})(\mathbf{u}_{con} + \mathbf{u}_{dis} + \mathbf{d}) + Z(\mathbf{x})K(\mathbf{x})\mathbf{x}\right] \\ &= -s^T\left[Z(\mathbf{x})(\mathbf{u}_{dis} + \mathbf{d})\right] \\ &= -s^T\left(\eta + \gamma_0 \left\|Z(\mathbf{x})\right\| + \right. \\ &\qquad \left. + \gamma_1 \left\|Z(\mathbf{x})\right\| \left\|\mathbf{x}\right\|\right) \mathrm{sgn}(s) + s^T Z(\mathbf{x})\mathbf{d} \\ &\le -\eta \left\|s\right\|_1 + \left\|Z(\mathbf{x})\right\| \left\|s\right\| \left\|\mathbf{d}\right\| - \\ &\qquad \left(\gamma_0 \left\|Z(\mathbf{x})\right\| + \gamma_1 \left\|Z(\mathbf{x})\right\| \left\|\mathbf{x}\right\|\right) \left\|s\right\|_1 \\ &\le -\eta \left\|s\right\|_1 + \left\|Z(\mathbf{x})\right\| \left\|s\right\| \left(\gamma_0 + \gamma_1 \left\|\mathbf{x}\right\|\right) - \\ &\qquad \left(\gamma_0 \left\|Z(\mathbf{x})\right\| + \gamma_1 \left\|Z(\mathbf{x})\right\| \left\|\mathbf{x}\right\|\right) \left\|s\right\|_1 \\ &\le -\eta \left\|s\right\|_1 + \left\|Z(\mathbf{x})\right\| \left(\gamma_0 + \gamma_1 \left\|\mathbf{x}\right\|\right) \left\{\left\|s\right\| - \left\|s\right\|_1\right\} \end{aligned} \tag{32}$$

where $\left\|s\right\|_1$ denotes 1-norm, and as $\left\|s\right\|_1 \ge \left\|s\right\|$, we have $\left\{\left\|s\right\| - \left\|s\right\|_1\right\} \le 0$. As a result, $\dot{V} = s^T \dot{s} \le -\eta \left\|s\right\| < 0$ for $\left\|s\right\| \ne 0$. It can be concluded from Theorem 3 that the states of the uncertain system (3) with ROSMC (30) are driven onto the sliding surface (28) at a finite time and remain on the surface, even when there are some internal parameter variations, external disturbances and parameter variations in the system. Also, sliding motion can minimize quadratic performance index (5). In other words, the designed system by ROSMC (30) is robust and optimal.

The block diagram of the designed ROSMC is presented in Fig. 4.

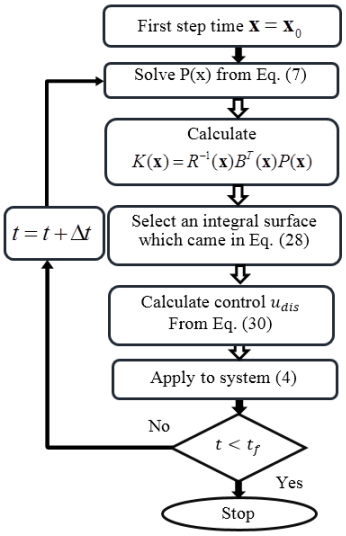

Fig. 4. Flowchart of the designed ROSMC.

6. Simulation Results

In this section, we simulate the results of all three methods using MATLAB software. The numerical values of system parameters for simulation are given in table I. It should be mentioned that since the given system is practical, there are always some input constraints in practice. Because of the difficulties, in this case, we have not considered the input saturation in the design procedure. However, we consider that in the simulation. It is assumed that the upper and lower bounds on the magnitude of the forces are $f_{1\max} = f_{2\max} = 50N$ and $f_{1\min} = f_{2\min} = -50N$ respectively. The sample time is chosen as $\Delta t = 0.001$ the second. Simulation is run from the initial time $t_0 = 0$ sec to the final time $t_f = 20$ sec. The initial conditions of the system are chosen as follows

$$\mathbf{x}(0) = \left[-0.2 \quad 0.25 \quad -\pi/6 \quad 0.1 \quad -\pi/6 \quad 0\right]^{\mathrm{T}}$$

The value of parameters $r_1, \cdots, r_4$ for inside and outside sectors in (26) are selected according to the upper bound value of the disturbances in scenario 1 and scenario 2 as $r_1 = 20, r_2 = 0$ and $r_3 = 20$, $r_4 = 0$. ROSMC' parameters in (30) are given as

$$M = \begin{bmatrix} 1 & 1 & 1 & 1 & 1 & 1 \\ 0 & 0 & 0 & 0 & 0 & 1 \end{bmatrix}, \begin{cases} \eta = 0.5 \\ \gamma = 0.05 \\ \delta = 10 \end{cases}$$

The function $\tanh(\cdot)$ is used instead of function $\mathrm{sgn}(\cdot)$ in (26) and (30). The weighting matrices Q, R, and F are chosen arbitrarily and are given in Table II.

Remark 4. The value of parameters $r_1, \cdots, r_4$ can be selected more significantly, but it increases the control signal unnecessarily. Also, the matrices Q and R can be used as design parameters to penalize the control signals

and the state variables. The larger these values are, the more you penalize these signals. Choosing a significant value for R means you try to stabilize the system with less (weighted) energy. On the other hand, choosing a small value for R means you do not want to penalize the control signal.

Table I. Parameter values for the system model [1].

Parameter	Value
m_g	0.46 kg
m_x	4.9 kg
m_y	8.9 kg
L	0.12 m
J	0.05 kgm2
η	1.2 Nsm^{-1}
g	9.81 ms^{-2}

Table II. Weighting matrices required for all controllers

Weight matrices	**Value**
Q	$\text{diag}\{200,1000,0,0,0,0\}$
R	$\text{diag}\{1,10^{-3}\}$
F	$\text{diag}\{1,1\}$

In order to compare the three designed controllers and investigate the robustness property of each one, it is assumed that an external disturbance is applied. For this purpose, two scenarios are designed as follows:

Scenario 1. In this case, a pulse disturbance is applied as

$$\mathbf{d}(x,t) = d\begin{bmatrix}1 & 10\end{bmatrix}^T,\ d = u(t-8) - u(t-9) \qquad (33)$$

where $u(t)$ is the unit step function. Simulation results for three controllers are demonstrated in Figs. 5-7. Simulations are divided into two time periods: before applying the external disturbance and after applying it. For the first period (0 to 8 sec), settling time is investigated. Steady-state error is considered for the period after the external disturbance affects the system. For the total time of simulation, two different indices are examined.

The simulation results of the SDDRE Method are presented in Fig. 5. State trajectories x, y and θ (a) and control effort (b) are given. As it can be observed, it is clear that the SDDRE law (6) provides good performance for the ducted fan engine. As shown in Fig. 5 (a) and Table III, output variables x and y regulate the desired value in less than 3.5 secs and 2.19 secs, respectively.

For the second period, i.e., after applying the disturbance, the outputs x and y do not regulate the desired value, and steady-state errors exist. As a result, the SDDRE method does not have the robustness property. Fig. 6 demonstrates the results for the VSC Method. As shown from Fig. 6 (a) and Table III, the output variable x regulates to the desired value in more than 8 sec, but the settling time for y is 1.8 sec. After applying the disturbance, the output x does not regulate the desired value, but y regulates with an acceptable steady-state error. Because of the variable structure in VSC design, there is some fluctuation in the output response x. Consequently, compared with SDDRE, the VSC method has better performance and robustness properties.

The simulation results for the ROSMC method are depicted in Fig. 7. According to Fig. 7(a) and Table III, contrary to the SDDRE and VSC methods, the state trajectories do not divert and remain on the desired value while applying the external disturbance on the system. Therefore, ROSMC provides optimal performance and robustness against uncertainties.

Two performance indices $J_{u_i} = \int |u_i(t)|\,dt$ for $i = 1,2$ and $J_{x_j} = \int |x_j(t)|\,dt$ for $j = 1,\cdots,3$ are used to compare optimality properties for three designed controllers. Results are given in Table IV. According to the results, both performance indices for ROSMC are minimum in comparison with the two others. Finally, for scenario 1, ROSMC has stronger robustness and much more optimality performance than SDDRE and VSC methods.

Scenario 2. In this scenario, a time-varying disturbance which is a nonlinear function of state variables is applied to the system

$$\mathbf{d}(x,t) = d\begin{bmatrix}1 & 10\end{bmatrix}^T,\ d = 3\sin^2 t + x_1^2 + x_2^2 \qquad (34)$$
$$8 \le t \le 9$$

Simulation results for three designs are shown in Figs. 8-9. Fig. 8 demonstrates state trajectories x, y and θ (a, b, c) respectively. Control efforts u_1 and u_2 are given in Fig. 6. According to Table V, the system performance in the presence of the external disturbance in all three methods are similar to previous scenarios.

The SDDRE method regulates the two outputs to zero in less than 3.5 seconds, but when the external disturbances affect the system, the values of the states are deviated from their final values, respectively. According to Table VI and Fig. 9, the index $J_1 = \int |u(t)|\,dt$ has the lowest value. The results show that the ROSMC has better performance in the presence of external disturbance. Thus, it can be concluded that the third method has optimal and robust performance against complex external disturbances.

7. Conclusions and Future Work

In this paper, we studied and compared three controller design methods for a ducted fan engine in the presence of disturbances. In the first design, a conventional SDDRE controller was proposed. The main objective of the proposed SDDRE method is to minimize a defined performance index. In this method, state variables of the system converge to zero very fast, but state responses deviate from their steady state when the external disturbances are considered. Thus, the main disadvantage of this design method is that it shows high sensitivity to disturbances. At the second design, an NTV sliding sector was proposed, based on which a variable structure controller (VSC) law was designed for a ducted fan engine. Although VSC law has good performance despite disturbances, the chattering phenomenon was observed in the system responses. As the final result, it was shown that the ROSMC method is robust against disturbances, and the performance index is optimized at the same time; also, there is no chattering or fluctuation in this approach.

Finite-time and arbitrary convergence time sliding mode control and integration with SDDRE technique to have optimal and robust performance for the given system will be the authors' future challenges.

8. Acknowledgments

This work was supported by Shahid Chamran University of Ahvaz under the grant number GN36267.

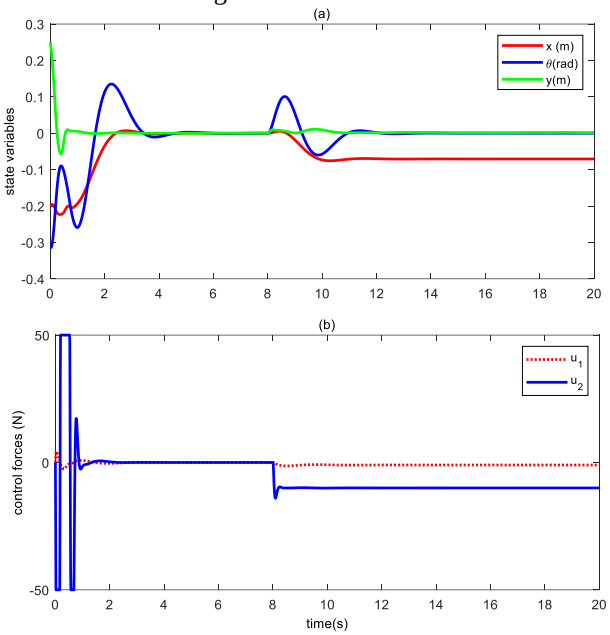

Fig. 5. Results of SDDRE for scenario 1. (a): State variables (x, y and θ). (b): Control inputs.

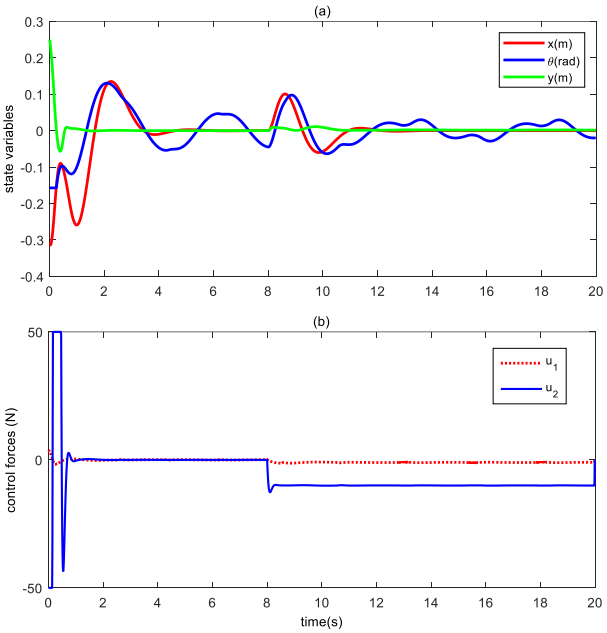

Fig. 6. Results of VSC for scenario 1. (a): State variables (x, y and θ). (b): Control inputs.

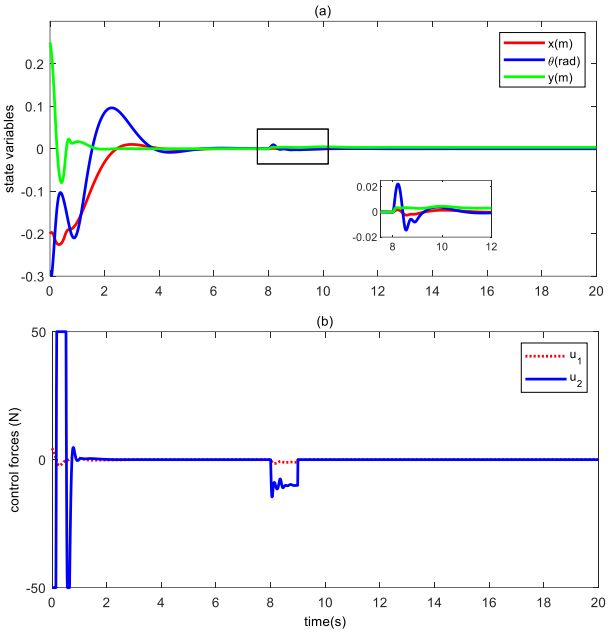

Fig. 7. Results of ROSMC for scenario 1. (a): State variables (x, y and θ). (b): Control inputs.

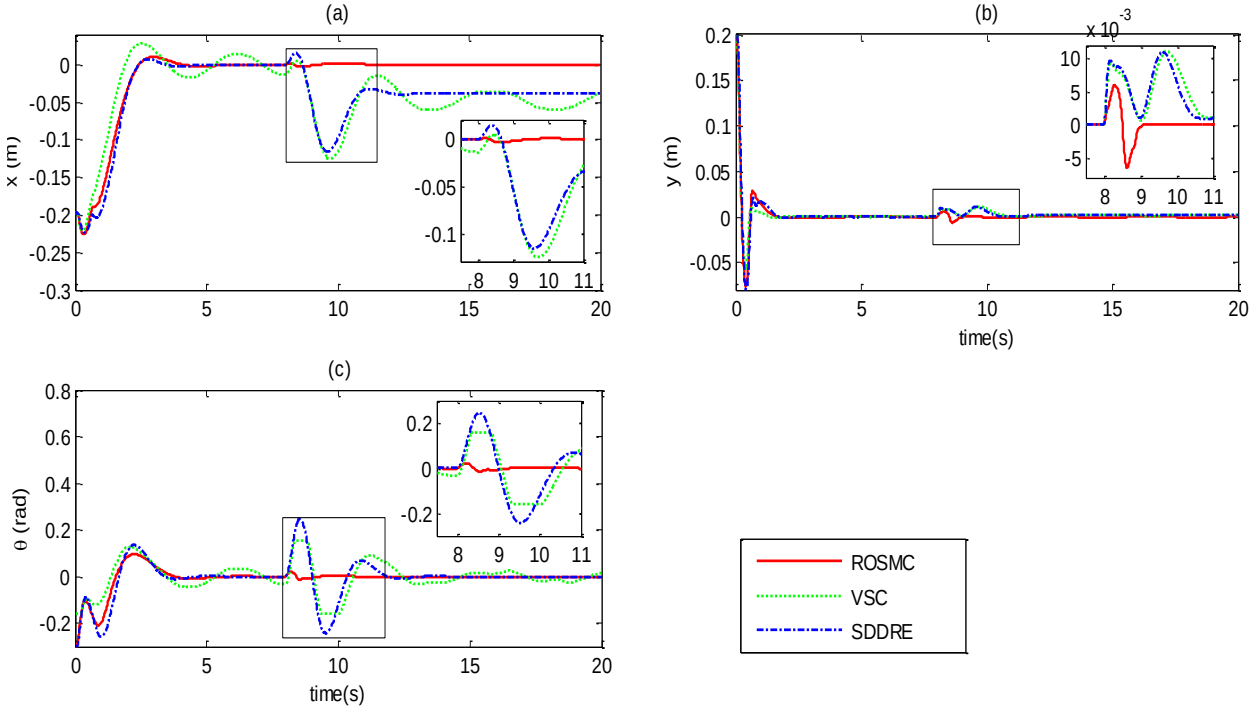

Fig. 8. Results of three designed controllers for scenario 2. (a), (b) and (c) state variables (x, y and θ).

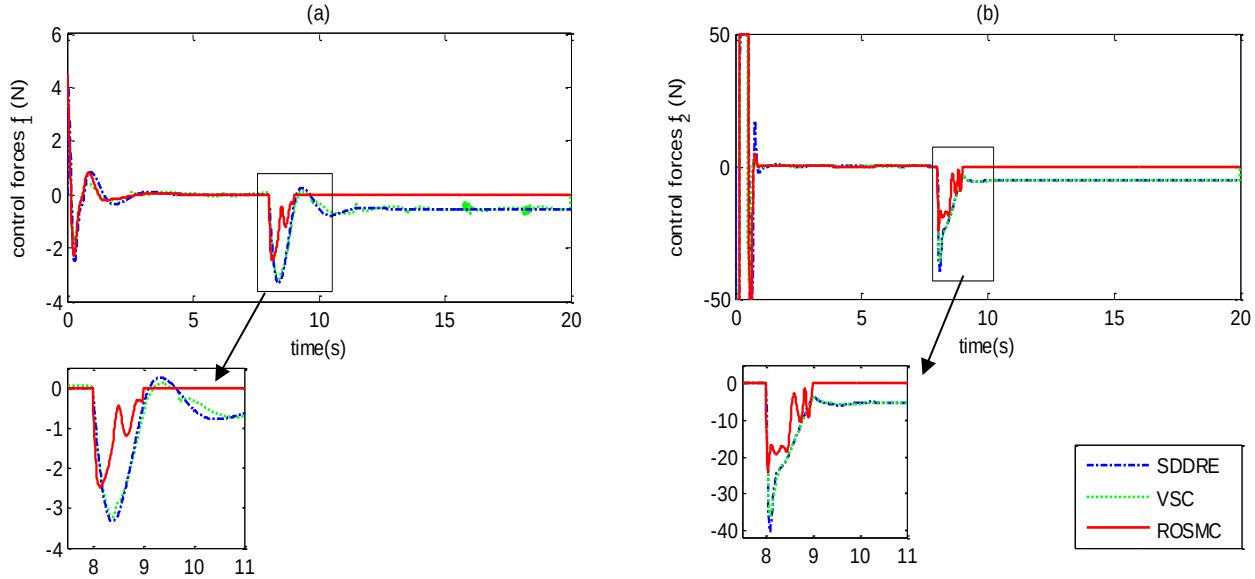

Fig. 9. Results of three designed controllers for scenario 2. (a), (b) and (c) control inputs.

Table III. Settling time and steady-state error for SDDRE, VSC, and ROSMC for scenario 1.

Control scheme	$\mathbf{t}_s^T = \begin{bmatrix} t_{sx} & t_{sy} \end{bmatrix}$	$\mathbf{e}^T = \begin{bmatrix} e_{xss} & e_{yss} \end{bmatrix}$
SDDRE	[3.51 2.19]	[0.0707 0.0031]
VSC	[8 1.8]	[0.0797 0.0025]
ROSMC	[3.8 1.4]	$[5.2\times10^{-8} \quad 9.6\times10^{-10}]$

Table IV. Performance indices for SDDRE, VSC, and ROSMC for scenario 1.

Control scheme	$\mathbf{J_u} = \begin{bmatrix} J_{u_1} & J_{u_2} \end{bmatrix}$	$\mathbf{J_x} = \begin{bmatrix} J_{x_1} & J_{x_2} & J_{x_3} \end{bmatrix}$
SDDRE	[13.7947 155.2545]	[1.1020 0.1060 05719]
VSC	[13.3524 148.2979]	[1.1933 0.0908 0.7185]
ROSMC	[2.4766 43.2747]	[0.3229 0.0650 0.3737]

Table V. Settling time, and steady-state error for SDDRE, VSC, and ROSMC for scenario 2.

Control Scheme	$\mathbf{t}_s^T = \begin{bmatrix} t_{sx} & t_{sy} \end{bmatrix}$	$\mathbf{e}^T = \begin{bmatrix} e_{xss} & e_{yss} \end{bmatrix}$
SDDRE	[4.55 2.22]	[0.037 0.0016]
VSC	[8.22 2.09]	[0.05 0.0019]
ROSMC	[3.85 1.85]	$[7.9\times10^{-8} \quad 6.0\times10^{-10}]$

Table VI. Performance indices for SDDRE, VSC, and ROSMC for scenario 2.

Control scheme	$\mathbf{J_u} = \begin{bmatrix} J_{u_1} & J_{u_2} \end{bmatrix}$	$\mathbf{J_x} = \begin{bmatrix} J_{x_1} & J_{x_2} & J_{x_3} \end{bmatrix}$
SDDRE	[9.7148 112.3749]	[0.8491 0.0978 0.8433]
VSC	[9.1479 105.4375]	[0.9095 0.0838 0.9547]
ROSMC	[2.6873 45.4788]	[0.3248 0.0684 0.3846]

9. References

[1] S. B. Fazeli Asl, S. S. Moosapour, "Adaptive backstepping fast terminal sliding mode controller design for ducted fan engine of thrust-vectored aircraft," *Aerospace Science and Technology*, vol. 71, pp. 521-529, 2017.

[2] W. Fan, X. Changle, X. Bin, "Modelling, attitude controller design and flight experiments of a novel micro-ducted-fan aircraft", *Advances in Mechanical Engineering*, vol. 10, no. 3, pp. 1-16, 2018.

[3] Y. Wang, C. Xiang, Y. Ma, and B. Xu, "Comprehensive nonlinear modeling and simulation analysis of a tandem ducted fan aircraft," in *Guidance, Navigation and Control Conference (CGNCC), 2014 IEEE Chinese*, pp. 255-261: IEEE, 2014.

[4] M. Chadli, S. Aouaouda, H.-R. Karimi, and P. Shi, "Robust fault tolerant tracking controller design for a VTOL aircraft," *Journal of the Franklin Institute*, vol. 350, no. 9, pp. 2627-2645, 2013.

[5] T. Cimen, "State-dependent Riccati equation (SDRE) control: A survey," IFAC Proceedings Volumes, vol. 41, no. 2, pp. 3761-3775, 2008.

[6] J. Pearson, "Approximation methods in optimal control I. Sub-optimal control," International Journal of Electronics, vol. 13, no. 5, pp. 453-469, 1962.

[7] M. Korayem, S. Nekoo, "Finite-time state-dependent Riccati equation for time-varying nonaffine systems: Rigid and flexible joint manipulator control," *ISA transactions*, vol. 54, pp. 125-144, 2015.

[8] A. Heydari and S. N. Balakrishnan, "Approximate closed-form solutions to finite-horizon optimal control of nonlinear systems," in American Control *Conference (ACC), 2012*, 2012, pp. 2657-2662: IEEE.

[9] A. Heydari, S. Balakrishnan, "Path planning using a novel finite horizon suboptimal controller", *Journal of guidance, control, and dynamics*, vol. 36, no. 4, pp. 1210-1214, 2013.

[10] L.G. Lin, M. Xin, "Impact Angle Guidance Using State-Dependent (Differential) Riccati Equation: Unified Applicability Analysis", *Journal of Guidance, Control, and Dynamics*, vol. 43, no. 11, pp. 2175-2182, 2020.

[11] J. Ashish, A.J. Sinclair, "Nonlinear control for spacecraft pursuit-evasion game using the state-dependent Riccati equation method", *IEEE Transactions on Aerospace and Electronic Systems*, vol. 53, no. 6, pp. 3032-3042, 2017.

[12] Y. Pan, K. D. Kumar, G. Liu, and K. Furuta, "Design of variable structure control system with nonlinear time-varying sliding sector," *IEEE Transactions on Automatic Control*, vol. 54, no. 8, pp. 1981-1986, 2009.

[13] B. Xu, D. Zhou, and S. Sun, "Finite time sliding sector guidance law with acceleration saturation constraint," *IET Control Theory & Applications*, vol. 10, no. 7, pp. 789-799, 2016.

[14] M. Cucuzzella, G.P. Incremona, A. Ferrara, "Event-triggered variable structure control", *International Journal of Control*, vol. 93, no. 2, pp. 252-260, 2020.

[15] C. Hongmei, "Simulation Research on Ship Electric Propulsion Speed Regulation System Based on Variable Structure Control and FPGA", *Microprocessors and Microsystems*, In press, 2020.

[16] H. Tourajizadeh and S. Zare, "Robust and optimal control of shimmy vibration in aircraft nose landing gear," *Aerospace Science and Technology*, vol. 50, pp. 1-14, 2016.

[17] C. Pukdeboon and P. Kumam, "Robust optimal sliding mode control for spacecraft position and attitude maneuvers," *Aerospace Science and Technology*, vol. 43, pp. 329-342, 2015.

[18] E.-H. Zheng, J.-J. Xiong, and J.-L. Luo, "Second order sliding mode control for a quadrotor UAV," *ISA transactions*, vol. 53, no. 4, pp. 1350-1356, 2014.

[19] A. H. Korayem, S. R. Nekoo & M. H. Korayem, "Sliding mode control design based on the state-dependent Riccati equation: theoretical and experimental implementation", *International Journal of Control*, vol. 92, no. 9, pp. 2136-2149, 2017.

[20] A.H. Korayem, S.R. Nekoo, M. H. Korayem, "Optimal sliding mode control design based on the state-dependent Riccati equation for cooperative manipulators to increase dynamic load carrying capacity." *Robotica*, vol. 37, no. 2, pp. 321-337, 2019.

[21] R. Farkh, M. Ksouri, and F. Bouani. "Optimal Robust Control for Unstable Delay System," *Comput. Syst. Sci. Eng.*, vol. 36, no. 2, pp. 307-321, 2021.

[22] G. Pujol-Vazquez, S. Mobayen, and L. Acho. "Robust control design to the furuta system under time delay measurement feedback and exogenous-based perturbation," *Mathematics*, vol. 8, no. 12, pp. 21-31, 2020.

[23] G. Gkizas, "Optimal robust control of a Cascaded DC–DC boost converter," *Control Engineering Practice*, vol. 107, 2021.

[24] D. Xu, Q. Wang, and Y. Li. "Adaptive Optimal Robust Control for Uncertain Nonlinear Systems Using Neural Network Approximation in Policy Iteration," *Applied Sciences*, vol. 11, no. 5, 2312, 2021.

[25] S. Kiamini, A. Jalilvand, and S. Mobayen, "LMI-based robust control of floating tension-leg platforms with uncertainties and time-delays in offshore wind turbines via TS fuzzy approach," *Ocean Engineering* vol. 154, pp. 367-374, 2018.

[26] Y. Batmani, M. Davoodi, and N. Meskin, "Nonlinear suboptimal tracking controller design using state-dependent Riccati equation technique," *IEEE Transactions on Control Systems Technology*, vol. 25, no. 5, pp. 1833-1839, 2016.

[27] Y. Batmani, and S. Khodakaramzadeh., "Nonlinear estimation and observer-based output feedback control," *IET Control Theory & Applications*, vol. 14, no. 17, pp. 2548-2555, 2020.

[28] Y. Batmani, " Event-triggered Observer Design for Nonlinear Networked Control Systems," *Tabriz Journal of Electrical Engineering*, vol. 49, no. 1, pp. 71-77, 2019.

[29] M. Nazari, "State Dependent Riccati Equation based Model Reference Adaptive Control for Finite Duration Cancer Treatment by using a Mixed Therapy," *Tabriz Journal Of Electrical Engineering*, vol. 48, no. 1, pp. 369-380, 2018.